

LETTER • **OPEN ACCESS**

Effects of land surface model resolution on fluxes and soil state in the Arctic

To cite this article: Meike Schickhoff *et al* 2024 *Environ. Res. Lett.* **19** 104032

View the [article online](#) for updates and enhancements.

You may also like

- [A new data-driven map predicts substantial undocumented peatland areas in Amazonia](#)
Adam Hastie, J Ethan Householder, Eurídice N Honorio Coronado et al.
- [An assessment of recent peat forest disturbances and their drivers in the Cuvette Centrale, Africa](#)
Karimon Nesha, Martin Herold, Johannes Reiche et al.
- [Detailed height mapping of trees and buildings \(HiTAB\) in Chicago and its implications to urban climate studies](#)
Peiyuan Li and Ashish Sharma

ENVIRONMENTAL RESEARCH
LETTERS

LETTER

Effects of land surface model resolution on fluxes and soil state in the Arctic

OPEN ACCESS

RECEIVED
20 July 2023REVISED
25 June 2024ACCEPTED FOR PUBLICATION
8 July 2024PUBLISHED
30 August 2024

Original Content from
this work may be used
under the terms of the
[Creative Commons
Attribution 4.0 licence](#).

Any further distribution
of this work must
maintain attribution to
the author(s) and the title
of the work, journal
citation and DOI.

Meike Schickhoff^{1,*} , Philipp de Vrese¹ , Annett Bartsch² , Barbara Widhalm²  and Victor Brovkin¹ ¹ Max Planck Institute for Meteorology, Bundesstr. 53, 20146 Hamburg, Germany² b.geos, Industriestrasse 1, 2100 Korneuburg, Austria

* Author to whom any correspondence should be addressed.

E-mail: meike.schickhoff@mpimet.mpg.de**Keywords:** land surface modeling, permafrost, high resolution, ArcticSupplementary material for this article is available [online](#)**Abstract**

Arctic land is characterized by a high surface and subsurface heterogeneity on different scales. However, the effects of land surface model resolution on fluxes and soil state variables in the Arctic have never been systematically studied, even though smaller scale heterogeneities are resolved in high-resolution land boundary condition datasets. Here, we compare 210 km and 5 km setups of the land surface model JSBACH3 for an idealized case study in eastern Siberia to investigate the effects of high versus low-resolution land boundary conditions on simulating the interactions of soil physics, hydrology and vegetation. We show for the first time that there are differences in the spatial averages of the simulated fluxes and soil state variables between resolution setups. Most differences are small in the summer mean, but larger within individual months. Heterogeneous soil properties induce large parts of the differences while vegetation characteristics play a minor role. Active layer depth shows a statistically significant increase of +20% in the 5 km setup relative to the 210 km setup for the summer mean and +43% for August. The differences are due to the nonlinear vertical discretization of the soil column amplifying the impact of the heterogeneous distributions of soil organic matter content and supercooled water. Resolution-induced differences in evaporation fluxes amount to +43% in July and are statistically significant. Our results show that spatial resolution significantly affects model outcomes due to nonlinear processes in heterogeneous land surfaces. This suggests that resolution needs to be accounted in simulations of land surface models in the Arctic.

1. Introduction

Earth system modelling is moving towards km-scale resolutions (Satoh *et al* 2014, Korn *et al* 2022, Hohenegger *et al* 2023). Such a high spatial resolution seems particularly advantageous for Arctic land surface modelling, since Arctic land is characterized by a high surface- and subsurface heterogeneity. Topography, surface materials, vegetation, hydrological conditions, and soil properties vary significantly over space (van Cleve *et al* 1983, Viereck 1992, Torre Jorgenson *et al* 2013). Soil organic carbon in tundra environments shows high enough variation coefficients to belong to Earth's most varied soils (Siewert *et al* 2021). And greenhouse gas fluxes vary more

among Arctic land cover types than from year to year (Treat *et al* 2018). The spatial scale of Arctic heterogeneities is well below the traditional Earth system model resolutions of 100–300 km which are typically used to investigate Arctic terrestrial processes (Koven *et al* 2013, Kleinen and Brovkin 2018, McGuire *et al* 2018, Burke *et al* 2020, de Vrese and Brovkin 2021). On these traditional scales, only large-scale features are resolved such as big mountain ranges, large river deltas and large-scale biomes such as tundra or taiga. In contrast, on scales of 1–10 km, smaller mountains, local forests and grasslands can be resolved and differentiations between upland and lowland areas as well as between yedoma soils and younger sediments can be included. Also soil properties such as soil texture

and soil organic carbon content show a large heterogeneity on smaller scales. For example, 1 km topography and soil texture substantially improve simulated soil moisture and terrestrial water storage anomaly relative to broader scale input as shown with a land surface model for the mid-latitudes (Singh *et al* 2015). For the Arctic, regional biogeochemical models show an improvement in carbon flux estimates with higher resolution (Treat *et al* 2018, Lara *et al* 2020, Albuhaishi *et al* 2023).

This suggests that high-resolution land surface models are favourable for accurately simulating Arctic terrestrial processes. The main benefit of high-resolution land surface models are the high-resolution land boundary conditions for topography, vegetation and soil in which small-scale heterogeneities are resolved. In contrast, the model code itself does not change between resolutions of 100–300 km and 1–10 km since parametrizations cannot be reduced on these scales in land surface models, contrary to atmospheric models. The disadvantages of high-resolution models include the much larger computational costs. This makes the use of a case study favourable to investigate the potential of high resolutions. The outcome may support educated decision-making regarding the future development of pan-Arctic high-resolution land surface models. More specifically, the impact of land boundary conditions' spatial resolution on hydrological, vegetation and soil processes in the Arctic has never been systematically studied before even though high-resolution input includes small-scale heterogeneities and thus may feature much stronger gradients. Therefore, we employ a case study to investigate the question: 'What are the effects of high-resolution land boundary conditions on simulating Arctic terrestrial processes?' We develop a high-resolution setup of the land surface model JSBACH3, in which the land boundary conditions are resolved on a scale of 5 km for a case study in the Chersky region in eastern Siberia. The atmospheric forcing, in contrast, is in a low resolution (about 210 km) to focus the analysis solely on effects due to the high-resolution land boundary conditions. We compare the results with the output of the same model in a traditional Earth system model resolution of 210 km and thereby investigate whether resolution plays a role in simulating the interactions of hydrology, vegetation and soil in the Arctic. We also quantify which model parameters and processes exert control on the differences between high- and coarse resolutions.

2. Methods

The case study area is situated in eastern Siberia within the continuous permafrost zone and extends from 158.4°–162°E and 67.5°–69°N (supplements).

High-resolution model input data was introduced for the land boundary conditions comprising orography, soil and vegetation parameters (supplements). A soil parameter that is not employed by all land surface models, but very important in this context, is the Clapp and Hornberger parameter (CHP). It is used to describe soil hydraulic properties and corresponds to the inverse of the pore size distribution index. CHP is empirically estimated by suction wetness data and increases when moving from coarse to fine soil textures (Clapp and Hornberger 1978). Besides the hydraulic conductivity, it can also be used to determine the amount of supercooled water in the soil (Ekici *et al* 2014). The vegetation distribution is based on Copernicus Sentinel-1 and -2 data from 2018 and 2019. The landcover retrieval scheme by Bartsch *et al* (2019) has been adapted including advanced pre-processing (similar as in Bartsch *et al* 2021), re-calibration (Bartsch *et al* 2024) and grouping of classes at 10 m nominal resolution. We use the three plant functional types 'C3 grass', 'deciduous shrubs' and 'extratropical deciduous trees' in our model. Evergreen trees are neglected since they show a very scarce distribution in the case study area. All model input parameters are transferred from the original resolution to 5 km and 210 km resolution using linear conservative remapping.

The land surface model JSBACH3 is the land component of the global Earth System Model MPI-ESM (Giorgetta *et al* 2013). We use the model version 3.2 (Reick *et al* 2021) including permafrost soil physics and a SOM scheme ranging from the surface to three meters depth (de Vrese *et al* 2021). The soil is vertically resolved into 18 layers with differing thickness up to a maximum depth of 40 m including bedrock. 11 layers are located within the first three meters. We run the model in two different horizontal resolutions, in 1.88° which corresponds to 210 × 77 km in the case study area, and in 0.045° which corresponds to ca. 5 × 2 km. While we ran the model at these resolutions, we scaled the model output for the analysis to represent only the domain for which the initial parameters are valid, i.e. the study area. Please note that, in the following, we refer to the simulations according to the resolution they were run at—i.e. 210 and 5 km respectively, even though that this does not constitute the spatial coverage considered in the analysis. The temporal resolution is 30 min. We use a standalone setup, thus we do not include feedbacks to the atmosphere. The model is forced with meteorological data from the Global Soil Wetness Project Phase 3 (Dirmeyer *et al* 2006). We use 1.88° forcing resolution for both horizontal resolution setups to investigate solely effects due to the land boundary conditions, and not effects due to the atmospheric forcing. The spin-ups span over the historical period from 1901 to 1979 and the analysis period encompasses 1980–2009 (Schickhoff *et al* 2024).

We compute resolution effects of variable X as

$$RE_X = \frac{(X_{5\text{km}} - X_{210\text{km}}) \cdot 100}{|X_{210\text{km}}|} \quad (1)$$

where variable X is averaged over the case study area and over the time period indicated. This gives relative differences to allow comparing resolution effects between different variables. For soil temperatures relative differences are not intuitive and instead absolute differences

$$aRE_X = X_{5\text{km}} - X_{210\text{km}} \quad (2)$$

are calculated. In addition to the control simulations with resolution effects RE_X^{control} , we use a set of idealized simulations to investigate the importance of individual parameters or sets of parameters (to test for synergetic effects). In these simulations, the parameters are individually set to a spatially uniform value in both resolution setups to remove any effect of the respective spatial heterogeneity. Here, the spatial average of the input parameter is used, calculated over the whole case study area. The resolution effects in these simulations RE_X^{uniform} are then compared to those in the control simulations:

$$\Delta RE_X = RE_X^{\text{control}} - RE_X^{\text{uniform}}, \quad (3)$$

to isolate the effects due to the heterogeneity of parameter X . We calculate ΔRE_X for every single input parameter individually to test their effects (supplements) and did not make parameter choices beforehand. To estimate if the differences between resolutions are statistically significant, two-tailed student's t -tests at 5% significance level against the interannual variability are applied over case study area averages of the time periods indicated. T -tests are adapted to account for autocorrelation (Zwiers and von Storch 1995, Lorenz *et al* 2016).

3. Results

3.1. Resolution effects of vegetation and soil parameters

Resolution effects on fluxes and soil state variables are present in the control simulations (table 1). In the summer mean, ALD resolution effects are large and statistically significant. Resolution effects in other variables are small, solely soil temperature also shows statistically significant differences. In July, evaporation resolution effects RE_{evap} equal +43% and are statistically significant. ALD and soil temperature show statistically significant differences in July and August, with RE_{ALD} amounting to +43% for ALD in August. Transpiration, drainage and GPP do not exhibit statistically significant differences due to smaller differences and large interannual variability. Overall resolution effects are largest in July.

Resolution effects of further variables such as soil ice and soil moisture, runoff, latent heat flux, sensible heat flux, soil heat conductivity and soil heat capacity are small (supplements).

Simulations with spatially uniform vegetation parameters show mostly small to negligible differences ΔRE for both the summer mean and July (table 2, for June and August see supplements). In contrast, simulations with spatially uniform soil parameters reveal much larger differences ΔRE . This shows that soil heterogeneity is more important regarding resolution than vegetation properties. The sum of ΔRE with uniform vegetation parameters and ΔRE with uniform soil parameters do not equal the total resolution effects, since synergistic effects occur. Simulations with spatially uniform elevation and orographic standard deviation show negligible differences ΔRE (supplements). An investigation of processes inducing the resolution effects is presented here for the variables ALD and evaporation, since they show very large and statistically significant resolution effects in July (evaporation) resp. August (ALD). The remaining variables are discussed in the supplements.

3.2. Effects on active layer depth

ALD shows substantial and statistically significant resolution effects RE_{ALD} . They increase from June to August as the active layer deepens with the longer thawing period. In the 5 km setup, the deepest ALDs occur in the southern mountain range (figure 1). The soils in this area hold very little SOM. Clay soil regions, characterized by high CHP values, also exhibit slightly deeper ALDs than average. SOM and CHP are the main drivers of ALD resolution effects. When setting them to spatially uniform, ΔRE_{ALD} amounts to +19% for SOM and to +15% for CHP in August (supplements). Setting both parameters uniform simultaneously gives ΔRE_{ALD} equal to +40% in August.

Heterogeneous SOM induces resolution effects due to its impact on the soil heat conductivity and on soil moisture, which in turn influences heat capacity, heat conductivity and the soil ice content. The dry and saturated soil heat conductivities both depend on the ratio of soil organic and mineral fractions. Mineral soils have a higher heat conductivity than organic soils due to two reasons. First, mineral particles such as sand, silt and clay have a higher heat conductivity than organic particles. Second, organic soils have a high porosity and thus a big pore volume. The air within the soil pores decreases the heat conductivity since air is a poor thermal conductor. Thus, soils with little SOM have a higher dry soil heat conductivity than soils with much SOM. Moreover, soil moisture plays a role since it affects the soil heat conductivity. Soils with high SOM characteristically store more absolute moisture than soils with little SOM, since the big pore volume gives much potential room for

Table 1. $RE_X^{control}$ signify the resolution effects between the two control simulations in 5 km and in 210 km resolution for the respective variables. They are calculated as the differences of the 5 km simulation relative to the 210 km simulation of 1980–2009 mean case study area averages [%] (equation (1)). Bold font indicates statistically significant differences between resolutions. Soil temperature difference refers to temperature in 19 cm depth [$^{\circ}C$] (equation (2)). Transp. refers to transpiration, ALD to active layer depth and GPP to gross primary productivity.

	ALD (%)	Drainage (%)	Evaporation (%)	GPP (%)	Soil temp. ($^{\circ}C$)	Transp. (%)
$RE_X^{control}$ JJA	+20	+0.8	+5.5	+4.8	+0.34	+3.3
$RE_X^{control}$ June	+1.7	+12	-3.8	-8.0	+0.3	+22
$RE_X^{control}$ July	+12	-7.1	+43	+13	+0.2	+21
$RE_X^{control}$ August	+43	+7.4	+13	+1.4	+0.5	-7.6

Table 2. Resolution effects of simulations with uniform parameters represented as the difference $\Delta RE_X = RE_X^{control} - RE_X^{uniform}$ for the respective variables [%] (equation (3)). Uniform parameters (all vegetation parameters resp. all soil parameters) are represented in the lines and output variables in the columns. The upper part of the table refers to the 1980–2009 summer mean and the lower part to 1980–2009 July mean. June and August are shown in the supplements. Soil temperature difference refers to temperature in 19 cm depth [$^{\circ}C$]. Transp. refers to transpiration, ALD to active layer depth and GPP to gross primary productivity. Veg. refers to vegetation.

JJA	ALD (%)	Drainage (%)	Evaporation (%)	GPP (%)	Soil temp. ($^{\circ}C$)	Transp. (%)
ΔRE_X veg. parameters	+2.3	+3.2	-0.5	-1.6	+0.03	-3.4
ΔRE_X soil parameters	+20	-2.3	+6.4	+7	+0.31	+7.2
July	ALD (%)	Drainage (%)	Evaporation (%)	GPP (%)	Soil temp. ($^{\circ}C$)	Transp. (%)
ΔRE_X veg. parameters	+2.2	+0.9	+6.1	-1.5	+0.03	-3.1
ΔRE_X soil parameters	+12	-8.1	+42	+15	+0.19	+24

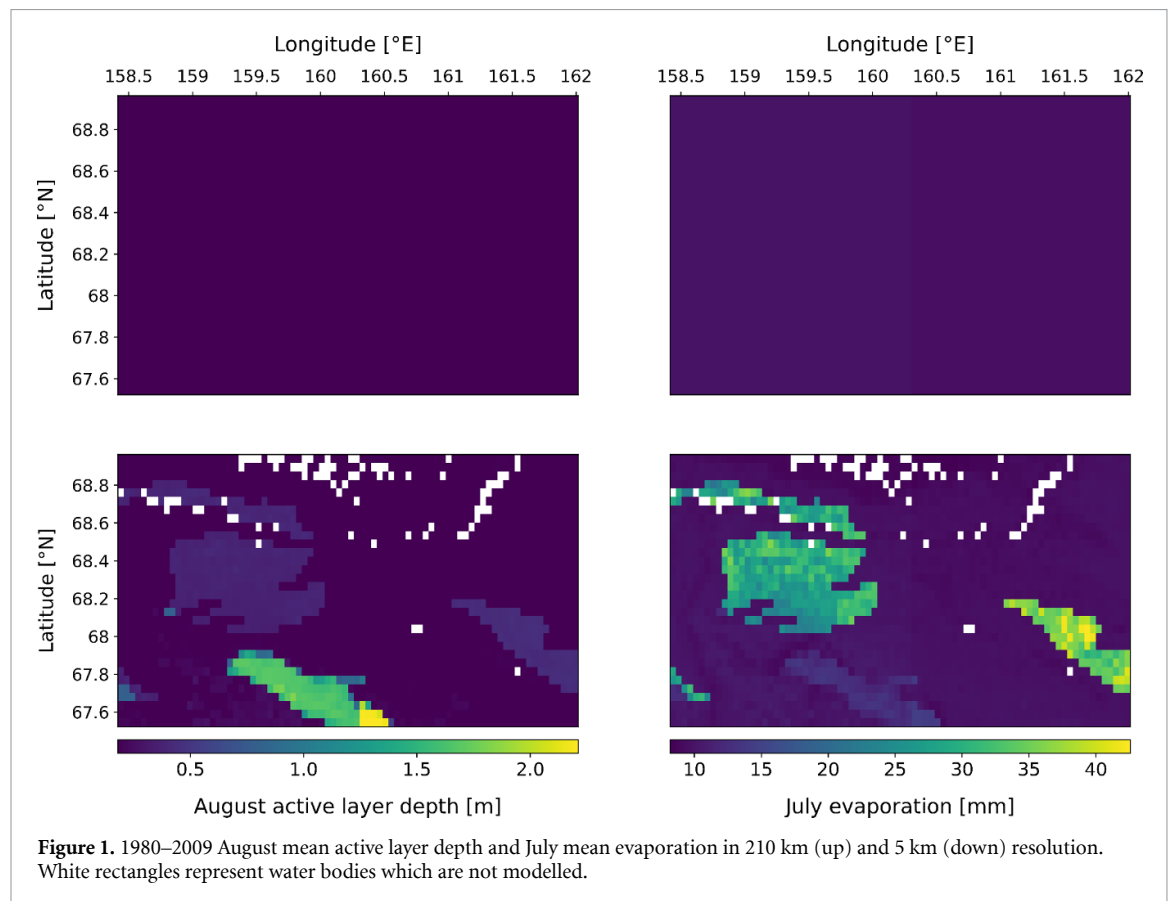


Figure 1. 1980–2009 August mean active layer depth and July mean evaporation in 210 km (up) and 5 km (down) resolution. White rectangles represent water bodies which are not modelled.

filling with water. However, due to the big potential space, these soils tend to have a lower soil saturation degree in the model. In contrast, soils with small SOM usually show a higher saturation degree due to the model parametrisations. In the case study area, the soils in the mountain range have very low amounts of

SOM and thus high saturation degrees. This reflects in deeper ALDs, because more saturated soils are better heat conductors than dry soils. In summer, the heat coming from above is well conducted to lower soil layers in the more saturated soils and leads to deeper ALDs. The heat conductivity of the first soil layer is

thereby determining for the amount of energy transferred from the surface to the soil. The soil saturation degree sat is calculated as follows:

$$sat = \frac{water_{soil} + ice_{soil}}{d_{soil} \cdot porosity} \quad (4)$$

with $water_{soil}$ being the absolute water content of the soil layer, ice_{soil} the absolute ice content of the soil layer, d_{soil} the soil layer depth and $porosity$ the volumetric porosity of the mixed mineral and organic soil. The total heat conductivity λ_{tot} of the respective soil layer is calculated as:

$$\lambda_{tot} = \lambda_{sat} \cdot Ke + \lambda_{dry} \cdot (1 - Ke) \quad (5)$$

with λ_{sat} being the heat conductivity of saturated soil and λ_{dry} the heat conductivity of dry soil. The Kersten number equals $Ke = \log_{10}(sat) + 1$ for $sat > 0.1$ and $Ke = 0$ for $sat < 0.1$.

Porosity decreases with decreasing SOM. A lower porosity leads to a higher saturation degree, because it is in the denominator of equation (4). A higher saturation degree causes a higher Kersten number and thus a higher total heat conductivity λ_{tot} , since the heat conductivity of saturated soils is much larger than the heat conductivity of dry soils due to water being a better heat conductor than air. Moreover, as explained above, both dry soil and saturated soil heat conductivities depend themselves on the ratio of mineral and organic soil fractions. Both increase with decreasing organic matter fractions. A higher total heat conductivity induces warmer soil temperatures and deeper ALDs. Therefore, low SOM is associated with deep ALDs. Notably, the ALD does not depend linearly on the SOM. SOM larger than 18% correspond to a mean ALD of 22 cm with a maximum of 81 cm, while SOM smaller than 14% are associated with ALDs of at least 80 cm to a maximum of 221 cm and a mean value of 158 cm.

Resolution effects induced by CHP also act via soil moisture differences. High CHP values correspond to high amounts of supercooled water in the soils. Due to much supercooled water, less soil ice is present and less energy is required for phase changes in spring. Thus, a larger part of the available energy goes directly into soil temperature increase and induces deeper ALDs. Moreover, the sum of soil moisture and soil ice within the first soil layer is largest where high CHP values are present. Thus, the numerator in equation (4) is large. The saturation degree is therefore higher than average and thus the heat conductivity is higher. Also the heat capacity is high due to the higher heat capacity of liquid water than of ice. A higher heat capacity increases the fraction of melting ice and contributes to deeper ALDs. In the 5 km setup, the August ALD amounts to 42 cm where CHP is high, while it amounts to only 24 cm in the average soil.

The annual cycle of ALD exhibits distinct behaviors in the two setups (figure 2(a)). The 210 km simulation stops thawing at 19 cm soil depth, which equals the second soil layer depth. This soil layer is considerably thicker than the first soil layer and thus holds more soil ice. All available energy goes into soil ice thawing, maintaining the temperature of the second soil layer at 0 °C throughout the summer. In contrast, some grid cells in the 5 km setup have more energy available and thaw beyond the second soil layer. On average, the soil thaws up until 28 cm depth in August in the 5 km setup. The key factor for the different behaviour in the two setups is the discrete treatment of the soil thermal processes, in which a soil layer of a given thickness is represented by a single set of variables, i.e. temperature, ice content etc. Thus, there is only one temperature per soil layer available which makes thawing of the respective layer binary and not gradual. The soil column is characterized by a nonlinear vertical discretisation (figure 2(b)). Soil layers close to the surface are thinner than soil layers situated deeper in the soil column. Larger amounts of pore ice in thicker soil layers require more energy to thaw than ice in thinner soil layers so the zero curtain period lasts longer. If one grid cell is thawed until the first soil layer and one until the third, the mean active layer depth does not equal the second soil layer active layer depth due to differing soil layer thicknesses. Thus, the soil does not thaw linearly according to SOM and CHP, but the soil layer discretisation introduces nonlinearity.

In summary, SOM and CHP induce spatial differences in soil heat conductivities. The nonlinear vertical discretization of soil layers and the discrete treatment of soil thermal processes amplify these differences nonlinearly, so they do not average out over space and produce resolution effects.

3.3. Effects on evaporation

Evaporation resolution effects are small when averaged over the whole summer (+5.5%), but large and statistically significant in July (+43%). In July, evaporation fluxes amount to 13.8 mm in 5 km and to 9.7 mm in the 210 km setup. Evaporation occurs from wet surfaces on vegetation and bare ground (skin evaporation), from the top soil layer (soil evaporation) and from snow. Snow evaporation is negligible in July. Skin evaporation comes to 8.9 mm in both resolution setups. It thereby makes up the largest share of total evaporation, but it does not induce resolution effects since the amounts are equal in both setups. Skin evaporation is computed by multiplying the fraction of wet surfaces with potential evaporation. The fraction of wet surfaces depends heavily on precipitation, but also upon the leaf area index and the maximum vegetated fraction of the grid box. The vegetation-dependence does not induce resolution effects, since the differences in fractions across

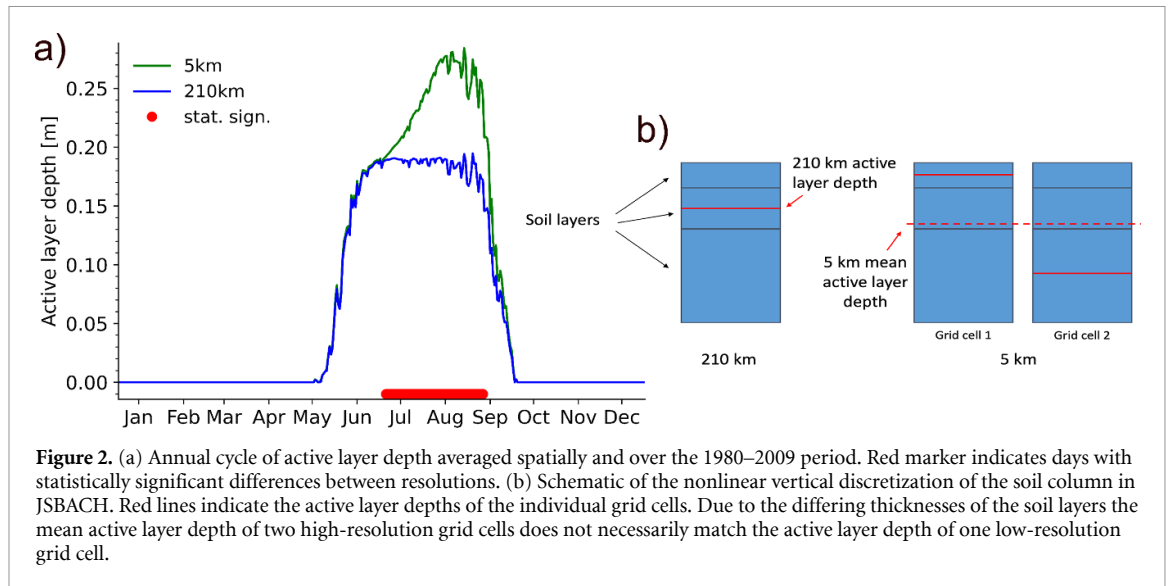


Figure 2. (a) Annual cycle of active layer depth averaged spatially and over the 1980–2009 period. Red marker indicates days with statistically significant differences between resolutions. (b) Schematic of the nonlinear vertical discretization of the soil column in JSBACH. Red lines indicate the active layer depths of the individual grid cells. Due to the differing thicknesses of the soil layers the mean active layer depth of two high-resolution grid cells does not necessarily match the active layer depth of one low-resolution grid cell.

the case study area are not large and balance out over the area. Precipitation is in low resolution and thus does not cause resolution effects. Potential evaporation depends on the vapour pressure deficit, temperature and wind speed. Since these forcing variables are also resolved in low resolution, they do not induce resolution effects in skin evaporation. Soil evaporation amounts to 4.8 mm in the 5 km setup and to only 0.7 mm in the 210 km setup. Thus, soil evaporation induces the resolution effects. Soil evaporation depends on the relative humidity h at the surface by

$$h = 0.5 \cdot \left(1 - \cos \left(\pi \cdot \frac{\theta}{\theta_{cap}} \right) \right) \quad (6)$$

θ denotes the top layer soil moisture and θ_{cap} the soil field capacity. The equation depicts a nonlinear dependency on the top layer soil moisture. Figure 3 illustrates this relationship for July data. Evaporation increases nonlinearly with top layer soil moisture. The nonlinearity induces the resolution effects. In comparison, in the 210 km setup, the top layer soil moisture amounts to 0.013 m and 0.012 m in the two grid cells. The high soil moisture amounts are thus not represented in 210 km, which is why soil evaporation in the 210 km setup is significantly smaller than in the 5 km setup.

Figure 1 shows total July evaporation in the case study region. The areas with especially high evaporation fluxes are the clay soil areas. They are characterized by a very high top layer soil moisture which sustains high evaporation fluxes. Clay soils hold high CHP values and thus have high amounts of supercooled water. Supercooled water is assumed to be immobile in the soil. However, as soon as it warms above 0 °C, it is mobile and can move within the soil. Supercooled water is thus more quickly available for diffusion than soil ice, which needs to be thawed first. The water can diffuse from the moist thawing front

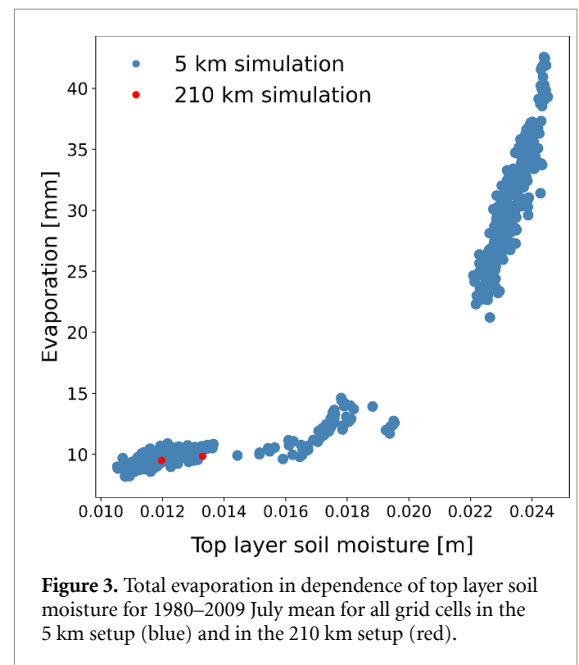


Figure 3. Total evaporation in dependence of top layer soil moisture for 1980–2009 July mean for all grid cells in the 5 km setup (blue) and in the 210 km setup (red).

in the second soil layer upwards to the top soil layer which is relatively drier. Moreover, CHP enters the equation to describe diffusion processes in the soil. High values increase the diffusion and provide more moisture supply. In simulations with uniform CHP values, ΔRE_{evap} amounts to 42%, while it is less than 6.5% for all other parameters.

4. Discussion

We show that there are model resolution effects on fluxes and soil state in the Arctic and that soil heterogeneity is the major player regarding resolution effects. Vegetation-induced resolution effects are minor in comparison. This is in alignment with a generally higher sensitivity of simulated water and

energy fluxes to soil input parameters than vegetation parameters (Li *et al* 2018). One factor for the smaller impact of vegetation are the setup of root depths in the model. They are not dependent on plant functional types, but distributed according to soil parameters (supplements). Here, however, it is highly plausible that effects due to plant-specific root depths would in any case be small, since the actual root depth in the study domain is limited to the active layer depths. Moreover, we hypothesize that in simulations with coupled land and atmosphere components, vegetation would have a larger effect on resolution due to feedbacks with the atmosphere. The albedo of trees and grasses is very different in winter, when snow is completely covering grasslands, but tree crowns stick out of the snow pack. Moreover, the differing roughness of trees and grasses influences the boundary layer turbulence and hence the land surface temperature. In the here conducted standalone simulations the land surface temperature is heavily dependent on the climate forcing and thus the impact of vegetation categories as defined for the model setup is small.

We further show that the resolution effects are induced by nonlinear characteristics of the model. The discrete treatment of soil thermal processes and the nonlinear vertical discretization of the soil column are most prominent and lead to resolution effects and differing behavior in ALD. We hypothesize that with a much finer vertical discretization of soil layers the resolution effects would decrease, because soil temperatures could change more continuously vertically. As shown for an inter-comparison of eight Arctic land surface models, the number of soil layers ranges from 3 to 30 for a depth of 2 m–47 m (Andresen *et al* 2020). The 18 layers utilized in this study are well within this range, however much more layers would be favourable to enable more gradual thawing.

We reveal that resolution effects due to SOM and CHP (determining the soil supercooled water amount) emerge to a large part due to impacts on the (relative) soil moisture distribution. This is in line with prior studies showing changes in modelled soil moisture with increasing resolution (Singh *et al* 2015, Ji *et al* 2017). This suggests that a good representation of (relative) soil moisture and more generally soil hydrology is important for high-resolution modelling. Furthermore, the sensitivity of model output to high-resolution soil input data indicates that high-quality soil data is required for future high-resolution land surface modelling. However, in particular for Arctic and boreal regions, observations are scarce and soil parameter estimates are often based upon remotely sensed landcover as proxy or upon traditional generalized soil maps. Input data thus often contains large uncertainties. Differences between the soil carbon stock maps SoilGrids, HWSO, and

NCSCD are especially large in boreal zones (Tifafi *et al* 2018). Significant soil carbon data gaps are present i.a. in the High Arctic, in high-latitude mountain and Yedoma regions (Hugelius *et al* 2014). Soil input data uncertainties are thus a potential source of error in high-resolution Arctic land surface modelling.

The generalisation of specific results from this study is limited by the use of only one land surface model and the coverage of only a small area. Different models may make different assumptions regarding the details of process representations such as the calculation of the soil heat conductivity (Dai *et al* 2019). This may lead to varying quantitative resolution effects between different land surface models, however the processes may be similar. Experiments with a different remapping method and a different initialisation routine show quantitative variations in resolution effects compared to the control simulations (supplements). However, the processes inducing the resolution effects stay the same and are robust against different remapping techniques and initialisation approaches. A comparison of JSBACH model output to observations was previously performed (Brovkin *et al* 2013, Dalmonech *et al* 2015, Schneck *et al* 2022), but not in this study. This study is aimed to conduct idealized simulations with the focus on process understanding regarding the effects of resolution and the sensitivity to gradients in the land boundary conditions.

5. Conclusion

We reveal differences between resolution setups in fluxes and soil state variables in the Arctic and show that these effects are primarily due to heterogeneous soil properties while vegetation characteristics play a minor role. Most effects are small in the summer mean, but larger within individual months. ALD presents large and statistically significant increases of +20% in the 5 km's summer mean relative to the 210 km setup and of +43% in August. There is a change in behavior between resolutions due to the nonlinear vertical discretization of the soil column amplifying impacts of soil parameter heterogeneity. July evaporation also features statistically significant differences between resolutions which equal +43%. SOM and CHP cause great shares of the resolution effects, largely by inducing spatial differences in (relative) soil moisture. Good high-resolution input data for soil parameters are thus necessary for high-resolution simulations, but they are limited by scarcity of observations in the Arctic. We show that spatial resolution matters for variables affected by nonlinear model characteristics. In order to make precise projections of future Arctic hydrology and permafrost carbon fluxes, effects of land boundary conditions' spatial resolution need to be considered.

Data availability statement

The full model output is available via the German Climate Computing Centre's long-term archive ([hdl:21.14106/00fad9c24fe67951ce4e0d07e0a4d90e85a5aa9e](https://hdl.handle.net/21.14106/00fad9c24fe67951ce4e0d07e0a4d90e85a5aa9e)). We use the model version JSBACH3.2 as presented in de Vrese *et al* (2021). The model code is freely available to the scientific community and can be provided by MPI-M. Analysis scripts can be obtained by contacting publications@mpimet.mpg.de.

Acknowledgments

We thank Zoé Rehder for comments on an earlier draft of this paper. We thank Mathias Goeckede for the provision of unpublished soil observational datasets and information about the case study region. We further thank Tobias Stacke and Veronika Gayler for technical support. The simulations were performed at the German Climate Computing Center (DKRZ). Vegetation input is based on modified Copernicus data from 2018 to 2019. This work was supported by the European Research Council project Q-Arctic (grant no. 951288), the European Space Agency CCI+ Permafrost project and by the German Research Foundation as part of the CLICCS Clusters of Excellence (DFG EXC 2037).

ORCID iDs

Meike Schickhoff  <https://orcid.org/0009-0001-1026-3504>
 Philipp de Vrese  <https://orcid.org/0000-0002-8813-7436>
 Annett Bartsch  <https://orcid.org/0000-0002-3737-7931>
 Barbara Widhalm  <https://orcid.org/0000-0002-4484-0947>
 Victor Brovkin  <https://orcid.org/0000-0001-6420-3198>

References

- Albuhaisi Y, van der Velde Y and Houweling S 2023 The importance of spatial resolution in the modeling of methane emissions from natural wetlands *Remote Sens.* **15** 2840
- Andresen C G *et al* 2020 Soil moisture and hydrology projections of the permafrost region—a model intercomparison *Cryosphere* **14** 445–59
- Bartsch A, Efimova A, Widhalm B, Muri X, von Baeckmann C, Bergstedt H, Ermokhina K, Hugelius G, Heim B and Leibman M 2024 Circumarctic land cover diversity considering wetness gradients *Hydrol. Earth Syst. Sci.* **28** 2421–81
- Bartsch A, Leibman M, Strozzi T, Khomutov A, Widhalm B, Babkina E, Mullanurov D, Ermokhina K, Kroisleitner C and Bergstedt H 2019 Seasonal progression of ground displacement identified with satellite radar interferometry and the impact of unusually warm conditions on permafrost at the Yamal Peninsula in 2016 *Remote Sens.* **11** 1–25
- Bartsch A, Pointner G, Nitze I, Efimova A, Jakober D, Ley S, Högström E, Grosse G and Schweitzer P 2021 Expanding infrastructure and growing anthropogenic impacts along Arctic coasts *Environ. Res. Lett.* **16** 115013
- Brovkin V, Boysen L, Raddatz T, Gayler V, Loew A and Claussen M 2013 Evaluation of vegetation cover and land-surface albedo in MPI-ESM CMIP5 simulations *J. Adv. Model. Earth Syst.* **5** 48–57
- Burke E J, Zhang Y and Krinner G 2020 Evaluating permafrost physics in the Coupled Model Intercomparison Project 6 (CMIP6) models and their sensitivity to climate change *Cryosphere* **14** 3155–74
- Clapp R B and Hornberger G M 1978 Empirical equations for some soil hydraulic properties *Water Resour. Res.* **14** 601–4
- Dai Y, Wei N, Yuan H, Zhang S, Shangguan W, Liu S, Lu X and Xin Y 2019 Evaluation of soil thermal conductivity schemes for use in land surface modeling *J. Adv. Model. Earth Syst.* **11** 3454–73
- Dalmonech D, Zaehle S, Schürmann G J, Brovkin V, Reick C and Schnur R 2015 Separation of the effects of land and climate model errors on simulated contemporary land carbon cycle trends in the MPI earth system model version 1 *J. Clim.* **28** 272–91
- de Vrese P and Brovkin V 2021 Timescales of the permafrost carbon cycle and legacy effects of temperature overshoot scenarios *Nat. Commun.* **12** 1–13
- de Vrese P, Stacke T, Kleinen T and Brovkin V 2021 Diverging responses of high-latitude CO₂ and CH₄ emissions in idealized climate change scenarios *Cryosphere* **15** 1097–130
- Dirmeyer P A, Gao X, Zhao M, Guo Z, Oki T and Hanasaki N 2006 GSWP-2: multimodel analysis and implications for our perception of the land surface *Bull. Am. Meteorol. Soc.* **87** 1381–97
- Ekici A, Beer C, Hagemann S, Boike J, Langer M and Hauck C 2014 Simulating high-latitude permafrost regions by the JSBACH terrestrial ecosystem model *Geosci. Model Dev.* **7** 631–47
- Giorgetta M A *et al* 2013 Climate and carbon cycle changes from 1850 to 2100 in MPI-ESM simulations for the Coupled Model Intercomparison Project phase 5 *J. Adv. Model. Earth Syst.* **5** 572–97
- Hohenegger C *et al* 2023 ICON-sapphire: Simulating the components of the Earth system and their interactions at kilometer and subkilometer scales *Geosci. Model Dev.* **16** 779–811
- Hugelius G *et al* 2014 Estimated stocks of circumpolar permafrost carbon with quantified uncertainty ranges and identified data gaps *Biogeosciences* **11** 6573–93
- Ji P, Yuan X and Liang X Z 2017 Do lateral flows matter for the hyperresolution land surface modeling? *J. Geophys. Res. Atmos.* **122** 12077–92
- Kleinen T and Brovkin V 2018 Pathway-dependent fate of permafrost region carbon *Environ. Res. Lett.* **13** 94001
- Korn P *et al* 2022 ICON-O: the ocean component of the ICON Earth system model—global simulation characteristics and local telescoping capability *J. Adv. Model. Earth Syst.* **14** 1–29
- Koven C D, Riley W J and Stern A 2013 Analysis of permafrost thermal dynamics and response to climate change in the CMIP5 earth system models *J. Clim.* **26** 1877–900
- Lara M J, Mcguire A D, Euskirchen E S, Genet H, Yi S, Rutter R, Iversen C, Sloan V and Wullschlegel S D 2020 Local-scale Arctic tundra heterogeneity affects regional-scale carbon dynamics *Nat. Commun.* **11** 4925
- Li J, Chen F, Zhang G, Barlage M, Gan Y, Xin Y and Wang C 2018 Impacts of land cover and soil texture uncertainty on land model simulations over the central Tibetan Plateau *J. Adv. Model. Earth Syst.* **10** 2121–46
- Lorenz R, Pitman A J and Sisson S A 2016 Does amazonian deforestation cause global effects; can we be sure? *J. Geophys. Res.* **121** 5567–84
- McGuire A D *et al* 2018 Dependence of the evolution of carbon dynamics in the northern permafrost region on the trajectory of climate change *Proc. Natl Acad. Sci. USA* **115** 3882–7

- Reick C H *et al* 2021 JSBACH 3—the land component of the MPI Earth system model: documentation of version 3.2 *Berichte zur Erdsystemforschung* **240**
- Satoh M *et al* 2014 The non-hydrostatic icosahedral atmospheric model: description and development *Prog. Earth Planet. Sci.* **1** 18
- Schneck R, Gayler V, Nabel J E, Raddatz T, Reick C H and Schnur R 2022 Assessment of JSBACHv4.30 as a land component of ICON-ESM-V1 in comparison to its predecessor JSBACHv3.2 of MPI-ESM1.2 *Geosci. Model Dev.* **15** 8541–59
- Schickhoff M, de Vrese P, Bartsch A, Widhalm B and Brovkin V 2024 JSBACH3.2 simulations of the Chersky region (Eastern Siberia) in the horizontal resolutions of 5 km and 210 km: control runs and idealized experiments (DOKU at DKRZ) (available at: www.wdc-climate.de/ui/entry?acronym=DKRZ_LTA_060_ds00009)
- Siewert M B, Lantuit H, Richter A and Hugelius G 2021 Permafrost causes unique fine-scale spatial variability across tundra soils *Glob. Biogeochem. Cycles* **35** 1–19
- Singh R, Reager J, Miller N and Famiglietti J 2015 Toward hyper-resolution land-surface modeling: the effects of fine-scale topography and soil texture on CLM4.0 simulations over the Southwestern U.S *Water Resour. Res.* **51** 2648–67
- Tifafi M, Guenet B and Hatté C 2018 Large differences in global and regional total soil carbon stock estimates based on soilgrids, HWSD and NCSCD: intercomparison and evaluation based on field data from USA, England, Wales and France *Glob. Biogeochem. Cycles* **32** 42–56
- Torre Jorgenson M *et al* 2013 Reorganization of vegetation, hydrology and soil carbon after permafrost degradation across heterogeneous boreal landscapes *Environ. Res. Lett.* **8** 035017
- Treat C C *et al* 2018 Tundra landscape heterogeneity, not interannual variability, controls the decadal regional carbon balance in the Western Russian Arctic *Glob. Change Biol.* **24** 5188–204
- van Cleve K, Dyrness C T, Viereck L A, Fox J, Chapin F S and Oechel W 1983 Taiga ecosystems in interior Alaska *BioScience* **33** 39–44
- Viereck L 1992 *The Alaska Vegetation Classification* 286 edn (US Department of Agriculture, Forest Service, Pacific Northwest Research Station)
- Zwiers F W and von Storch H 1995 Taking serial correlation into account in tests of the mean *J. Clim.* **8** 336–51